Annu. Rep. Nishi-Harima Astron. Obs. **22,** 6–16 (2012)

Polarimetry of Earthshine Using the 60cm Telescope of the Nishi-Harima Astronomical Observatory

Jun Takahashi, Yoichi Itoh

Nishi-Harima Astronomical Observatory, Center for Astronomy, University of Hyogo, 407-2 Nishigaichi, Sayo-cho, Sayo-gun Hyogo 679-5313, Japan

E-mail: takahashi@nhao.jp

and Takahiro Niwa

Hachinohe National College of Technology, 16-1 Uwanotai, Tamonoki, Hachinohe City, Aomori 039-1192, Japan

(Received 2012 December 29)

Abstract

The results of monochromatic (V band) polarimetry of Earthshine on the Moon are presented. The observations aimed to evaluate a polarization difference between Earthshine contributed by reflection at a land-dominant surface and an ocean-dominant surface. As viewing from Japan, we can observe Earthshine with contribution from a land-dominant surface in waxing phases of the Moon, whereas we can study that from an ocean-dominant surface in waning phases. We utilized a 60cm reflecting telescope at Nishi-Harima Astronomical Observatory and the simultaneous imaging/spectrometric polarimeter which enables a simultaneous measurement of four polarized components with a single exposure. In a series of observations from May 2010 to March 2012, twelve data sets were obtained for the waxing phases and seven data sets for the waning. The polarization degree increased as the Earth phase approaches to a quadrature. The maximum polarization degree was roughly $\sim$ 8 % for both phases, which is consistent with other recent polarimetric measurements. Fitting of a function for Rayleigh scattering yields the polarization maximum of 7.7$\pm$0.4% and 8.4$\pm$0.7% for the waxing and waning phases, respectively. Although a larger polarization by an ocean-dominant surface has been implied, the difference is not significant. The upper limit of the difference is $\sim$ 1% in Earthshine, which is interpreted as $\sim$ 3% in Earthlight.

Key words: Earthshine – Polarimetry – Extrasolar Planets – Ocean

1. Introduction

Liquid, whether water or not, seems to be important and favorable for existence of life (Benner, Ricardo, Carrigan, 2004). In the context of searching for extraterrestrial life, how can we find a planet which holds liquid? Polarimetry may provide a clue because specular reflection from a liquid surface produces higher polarization than reflection from a rough surface does.

This idea was proposed by some theoretical studies. McCullough (2006), though it was not published, calculated polarization from a model planet covered with an ocean surface and showed that it would be significantly larger than that with land, desert or snow. In his result, the maximum polarization degree for an ocean planet would be larger than that for other types of planets by at least 40% in case the atmosphere is cloud-free. If the planet was covered with clouds of Earth-like fraction, the difference would be $\sim$15-20%. Zugger et al. (2010) performed similar calculations with more detailed parameter variations. They suggested that polarization measurements in combination of regular photometric observations can be used to detect extrasolar oceans, aerosols and clouds.

Fig. 1. **Photograph of Earthshine:** This photograph is by courtesy of Mr. N. Tokimasa.

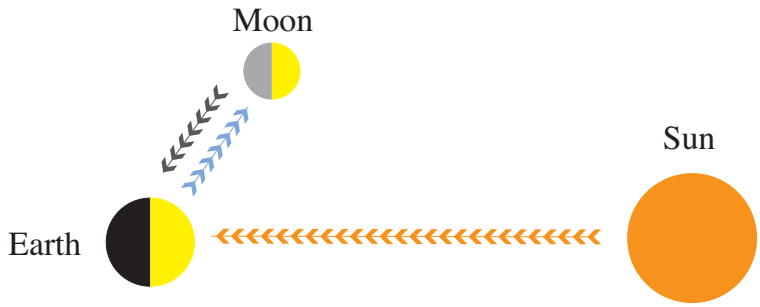

Fig. 2. **Schematic illustration of Earthshine occurrence:** Sunlight is reflected from the Earth surface. Then, part of the reflected light goes to the Moon and is reflected back to the Earth.

It is important to observationally confirm these theoretical calculations. However, it is not easy since we have yet to know any planet with an ocean surface other than the Earth. The aim of this study is to evaluate the polarization enhancement by an ocean surface using Earthshine polarimetry.

Earthshine is Earthlight reflected from the lunar surface; it appears as a faint glow on the dark side of the Moon (Fig. 1). As illustrated in Fig. 2, Sunlight is reflected from the Earth surface, then, part of the reflected light goes to the Moon, and finally it is reflected back to the Earth. Since Earthshine is originated from Earthlight, scientific observations of Earthshine have been made mainly with the intention either to know more about our planet itself or to test observations of an Earth-like extrasolar planet. Although many authors conducted photometry and spectrometry of Earthshine (see review papers Arnold, 2008; Pallé, 2010), there have been only a few projects of Earthshine polarimetry (Dollfus, 1957; Sterzik, Bagnulo, Palle, 2012; Takahashi et al., 2013). No polarimetry has been done for evaluation of the polarization enhancement by an ocean surface.

Observations from Japan is preferable for the purpose of this study. Japan is located on the border between a vast continent (Eurasia) and a huge ocean (the Pacific). Thus, Earthshine on the waxing Moon is contributed by a land-dominant Earth surface, whereas that on the waning Moon is originated from an ocean-dominant surface (Fig. 3). This circumstance allows us to compare polarization from different types of surfaces.

In addition, results from the polarimetric measurements of Earthshine during a lunar eclipse are also discussed in this paper. Note that in this paper, the light of the Earth as viewed from the space is referred to as *Earthlight*, which is distinguished from *Earthshine* on the Moon as observed from the ground.

[1] The standard stars were observed on 2010-09-01 (the night before)

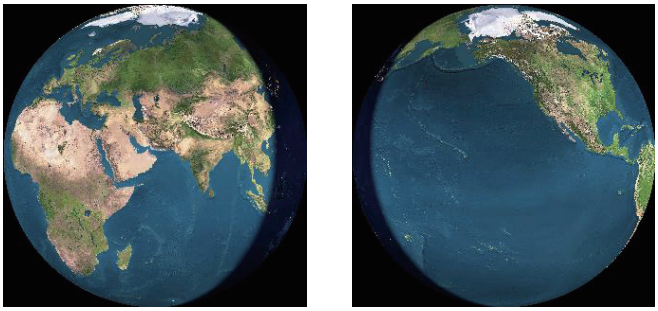

Fig. 3. **Earthshine contributing surfaces for the waxing crescent Moon at 2010-05-17 11:07 UT (left) and for the waning crescent Moon on 2010-06-09 18:51 UT (right):** The ocean coverages are $\sim$ 45% (left) and 80% (right). These images were produced with the Earth and Moon Viewer (http://www.fourmilab.ch/earthview/vplanet.html) .

Table 1. **Observational parameters** - α_e and N denote Earth phase angles and the directions normal to the scattering plane at the mid-time of observations, retrieved from NASA/JPL HORIZONS system (http://ssd.jpl.nasa.gov/horizons.cgi). The used unpolarized standard stars are θ UMa (U1), β UMa (U2), γ Boo (U3), HD154892 (U4), β Cas (U5), β Tau (U6) and γ Gem (U7). The used polarized standard stars are HD154445 (P1), HD161056 (P2), HD204827 (P3), ϕ Cas (P4) and HD21291 (P5).

Moon phase	Date (UT)	Start UT	End UT	α_e [deg]	N [deg]	Unpol. Std.	Pol. Std.
Waxing	2010-05-16	10:50	11:30	29.9	176.3	U1, U2, U3	P1, P2
	2010-05-17	10:32	11:42	42.9	4.3	U1, U2	P1, P2
	2010-05-20	10:42	11:32	82.8	19.1		
	2010-05-21	10:40	12:51	96.4	21.0		
	2011-10-04	10:52	12:47	93.8	173.9		
	2011-10-06	11:55	12:28	117.6	166.4		
	2011-10-31	09:40	11:04	61.9	175.1		
	2012-01-27	10:05	10:49	48.4	152.4	U6, U7	P4, P5
	2012-01-28	08:52	09:25	59.1	153.9		
	2012-01-29	11:14	11:16	70.9	156.2		
	2012-01-31	11:24	12:31	92.9	162.6		
	2012-02-01	10:39	11:37	103.7	166.5		
Waning	2010-06-03	16:47	19:14	102.8	158.8	U2, U3	P1, P2
	2010-06-09	18:23	19:19	34.4	168.0	U1, U2, U3	P1, P2, P3
	2010-09-02	15:21	18:51	77.2	177.4	U3, U4, U5[1]	P1, P2, P3[1]
	2011-09-22	17:36	18:54	63.0	9.0		
	2011-12-18	17:14	19:34	79.7	22.5		
	2011-12-19	18:26	20:28	65.9	20.2		
	2012-03-15	18:29	19:01	80.3	178.0		
Eclipse (east)	2011-12-10	13:00	15:03	179.4	97.2	U5, U6, U7	P3, P4, P5
Eclipse (west)	2011-12-10	14:00	14:58	179.4	83.3	U5, U6, U7	P3, P4, P5

2. Observations

We conducted polarimetry of Earthshine from May 2010 to March 2012 to cover a wide range of Earth phase angles (the Sun-Earth-Moon angles, α_e) in both of the waxing and waning Moon phases (Table 1). The observations were made with a 60 cm reflecting telescope at Nishi-Harima Astronomical Observatory (NHAO), located in Hyogo, Japan. The utilized instrument is a simultaneous imaging/spectrometric polarimeter, developed by Fujita et al. (2009) and Nishida (2008). The instrument obtains four polarized images simultaneously by using a non-polarized beam splitter and two Wollaston prisms. A half-wave plate, which rotates the oscillation angles of light beams by 45°, is placed before one of the Wollaston prisms. This configuration enables simultaneous measurement of Stokes parameters (Q and U), thus improves precision in degree of polarization (P) and position angle of polarization (Θ). It also saves time of observations thanks to fewer number of exposures and readouts. Earthshine observations, especially at crescent Moon phases, enjoy this benefit because they otherwise faced challenges arising from rapid arimass/background changes and short observable time.

The telescope was pointed to the celestial east and west edge of Earthshine on the waxing and waning Moon, respectively (Fig. 4a). The Moon moves east typically by $\sim 0.5'$/min in the equatorial coordinates. However the telescope is not able to track along the lunar movement but tracks along the stellar movement. As the typical exposure time was one minute, the obtained Earthshine images were blurred. An example of obtained image is shown in Fig. 4b.

As seen in Fig. 4b, the polarimeter projects four rectangular windows on a CCD chip. They correspond to F_0, F_{45}, F_{90}, and F_{135} images, where F_ψ represents the intensity of light beam in an oscillation angle of ψ degrees with respect to celestial north. The field of view (FOV) of each window is $\sim 2.2' \times 8.7'$ (Nishida, 2008). The long side of the image window was placed in the east-west direction. The pixel scale is $0.65''$/pixel (Nishida, 2008). The V band (centered at wavelength 551 nm) filter was installed in the instrument. The attached CCD was cooled by a temperature ~ 30 °C colder than the environment temperature (between 0 and 30 °C).

Dark frames were obtained every night. Flat frames were acquired by pointing the dome wall illuminated by the light from the top ring of the telescope. Unpolarized and polarized standard stars were observed every consecutive observations as far as possible. Those standard stars were selected from Hsu & Breger (1982), Turnshek et al. (1990), and Schmidt, Elston, Lupie (1992).

A lunar total eclipse took place on December 10, 2011, which provided us with a rare opportunity to observe Earthshine at $\alpha_e \sim 180°$. We observed Earthshine on the lunar eclipse at several areas on the Moon.

3. Data Reduction

3.–1. Subtraction of Sky Background

IRAF was used for the data reduction. After dark subtraction and flat fielding, the sky background was subtracted in the following method. The sky background around Earthshine is very strong due to the scattered light from Moonshine. Therefore its subtraction is very important. The four windows were aligned and trimmed in a manner such that all of the Earthshine images were at the same pixel positions. The offset values for the alignment were derived from the observations of the standard stars. The mean $((\sum_\psi F_\psi)/4)$ frame was generated from the trimmed four F_ψ frames. F_m frame is referred to as the mean frame.

Then the pixel values in each of F_ψ and F_m frames were averaged along the horizontal axis in Fig. 4b, which resulted in one-dimensional data along the vertical (x) axis (Fig. 5a). The 1D data of F_m was used to define Earthshine, sky and buffer regions. The occurrence of the buffer region is due to non-lunar (but stellar) tracking of the telescope. The blur boundary between Earthshine and sky in Fig. 4b is the buffer region. Connected three linear functions were fitted to the observational data by varying two free parameters: the central coordinate (X_c) and the half width (w) of the buffer region (Fig. 5a). The analyzed

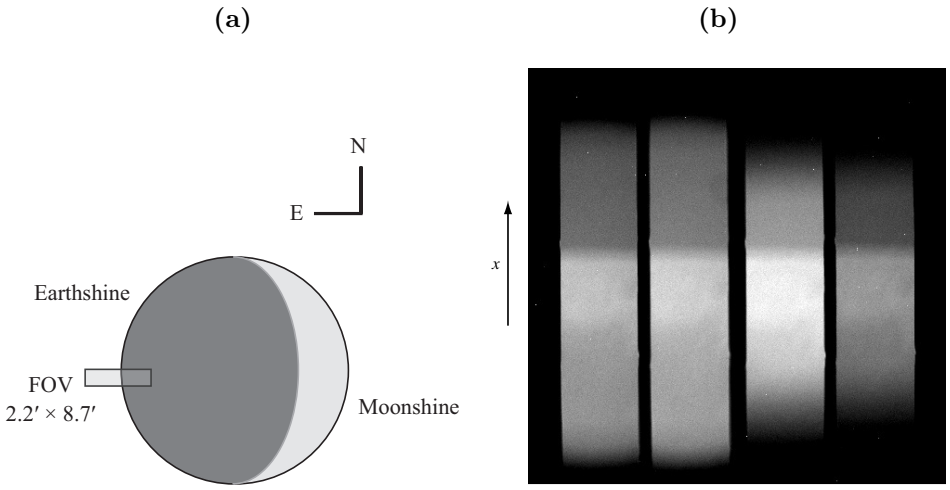

Fig. 4. **(a) FOV of Earthshine on the waxing Moon:** For waning Moon, Earthshine is located on the celestial west side of the Moon. **(b) Example of obtained raw images:** The four windows correspond to F_{135}, F_{45}, F_0, and F_{90} images from left, respectively. The lower side in each window is Earthshine and the upper side is sky. The upward direction in the image is east and the leftward direction is north. This image was taken on 2010 May 17.

pixel region is a range of 300-500 pixel wide, beginning at [5:300] and extending toward [450:650]. It was tuned for every date according to different stray light patterns. We regarded the definition of the regions for the least value of $\sum \left[(Obs.\ data) - (Fit\ line)\right]^2$ as the best definition.

The region definition derived from the F_m data were applied to all of the four F_ψ data (Fig. 5b). A linear function was fitted to the data in the defined sky region. The region for the fit begins from 15 pixel away (toward sky) from sky/buffer boundary and extends to the edge of the analysis region described above. The best-fit function was extrapolated toward the Earthshine region and subtracted from the data values. We averaged the subtracted data values sampled in the 50-pixel-wide area whose edge is located at a position 15 pixel away from the Earthshine/buffer boarder (Fig. 5b). In the procedure as described above, sky-subtracted values of F_ψ were derived.

3.–2. Correction for Instrumental Polarization

From the measured values of F_ψ, we have Stokes parameters:

$$q' = \frac{Q'}{I'} = \frac{F_0 - F_{90}}{F_0 + F_{90}}, \tag{1}$$

and

$$u' = \frac{U'}{I'} = \frac{F_{45} - F_{135}}{F_{45} + F_{135}}. \tag{2}$$

q' and u' should be corrected because they are suffered from instrumental (including telescope) polarization. Correction was made by assuming linear instrumental responses to input true Stokes parameters q and u:

$$\begin{pmatrix} q' \\ u' \end{pmatrix} = \begin{pmatrix} b_1 \\ c_1 \end{pmatrix} + \begin{pmatrix} b_2 & b_3 \\ c_2 & c_3 \end{pmatrix} \begin{pmatrix} q \\ u \end{pmatrix}. \tag{3}$$

Coefficients b_i and c_i $(i = 1, 2, 3)$ can be determined by observing unpolarized and polarized standard stars. Because $q = u = 0$ is known for unpolarized standard stars, b_1 and c_1 are directly determined by

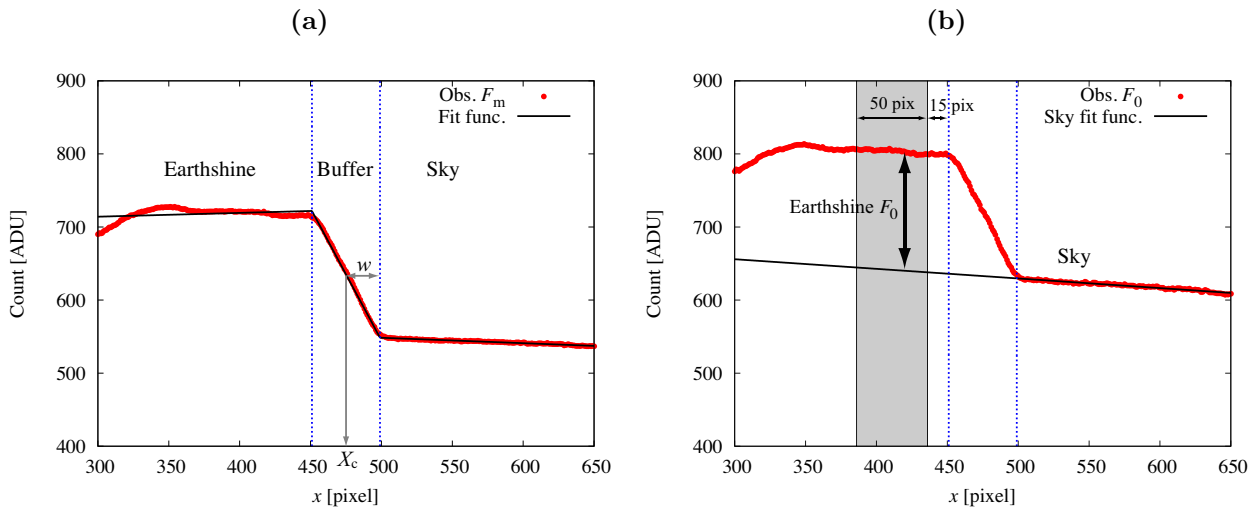

Fig. 5. **(a) Example of one-dimensional F_m data:** Connected three linear functions (solid lines) were fitted to the observational data (circles) in order to define Earthshine, buffer and sky regions. The central coordinate (X_c) and the half width (w) of the buffer region were varied to determine the best region division. This data is originated from the data of Fig. 4b. **(b) Example of one-dimensional F_0 data:** The region definition derived from F_m data was applied (divided by the vertical dot lines). A linear function was fitted to the data in the sky region and extrapolated toward the Earthshine region. Sky-subtracted F_0 values of Earthshine were sampled in the shaded area. This data is originated from the data of Fig. 4b.

their observations as

$$b_1 = q' \text{ and } c_1 = u'. \tag{4}$$

Because q and u for polarized standard stars are known, we can write simultaneous equations of b_2 and b_3 (c_2 and c_3) by observing two different polarized standard stars and measuring values of q' (u'). Solving the simultaneous equations yields

$$\begin{pmatrix} b_2 & c_2 \\ b_3 & c_3 \end{pmatrix} = \frac{1}{q_A u_B - q_B u_A} \begin{pmatrix} u_B & -u_A \\ -q_B & q_A \end{pmatrix} \begin{pmatrix} q'_A - b_1 & u'_A - c_1 \\ q'_B - b_1 & u'_B - c_1 \end{pmatrix}, \tag{5}$$

where variables with subscripts A and B represent values for different stars. When we succeeded to observe three different polarized standard stars, we obtained three set of (b_2, b_3, c_2, c_3). In this case, we averaged the three values. The averaged values of b_i and c_i are summarized in Table 2.

After obtaining all of the b_i and c_i, we can correct the instrumental polarization by

$$\begin{pmatrix} q \\ u \end{pmatrix} = \frac{1}{b_2 c_3 - b_3 c_2} \begin{pmatrix} c_3 & -b_3 \\ -c_2 & b_2 \end{pmatrix} \begin{pmatrix} q' - b_1 \\ u' - c_1 \end{pmatrix}. \tag{6}$$

3.–3. Derivation of P, Θ and their errors

Single exposure gives one set of q and u. We averaged the values of q and u from all the effective exposures at the night. Then, the degree of polarization (P) and position angle of polarization (Θ) were derived by

$$P = \sqrt{q^2 + u^2}, \tag{7}$$

$$\tan 2\Theta = \frac{\mathrm{u}}{\mathrm{q}}, \text{ and } \mathrm{sgn}\,[\cos 2\Theta] = \mathrm{sgn\,q}, \tag{8}$$

Table 2. **Correction parameters of the instrumental polarization** - The values are averaged over all the measurements.

Parameter	Value
b_1	-0.005 ± 0.002
b_2	1.01 ± 0.03
b_3	0.01 ± 0.09
c_1	0.007 ± 0.001
c_2	0.05 ± 0.04
c_3	1.01 ± 0.09

where sgn in Equation (8) stands for "sign of." Θ is defined in the region $0 \leq \Theta < 180$.

The errors of P and Θ were determined using the rule of error propagation:

$$\sigma_P = \frac{\sqrt{q^2\sigma_q^2 + u^2\sigma_u^2}}{P}, \tag{9}$$

$$\sigma_\Theta = \frac{90}{\pi}\frac{\sqrt{u^2\sigma_q^2 + q^2\sigma_u^2}}{P^2} \text{ [deg]}, \tag{10}$$

where σ_z represents the error of z. σ_q and σ_u equal one standard deviation of q and u, respectively.

4. Results and Discussion

4.–1. General Results

The results are summarized in Table 3. The derived values of P are shown in Fig. 6. Overall, P of Earthshine on both waxing and waning Moon increases with α_e increasing from ∼30° to ∼90°. P appears to be saturated in a range of α_e between 70° and 110°, though it is difficult to definitively determine the phase angle for the maximum degree of polarization due to large σ_P in $\alpha_e > 90°$. In general, errors in polarization measurements for Earthshine increases with increasing Earth phase angle because Earthshine brightness decreases and sky background increases due to brighter Moonshine. The maximum polarization seems to be ∼8%, omitting the results with largest σ_P in each of waxing and waning phases, namely results on 2011-10-06 ($P = 9.8 \pm 4.5\%$) and 2012-03-15 ($12.7 \pm 3.5\%$). This is consistent with our recent spectropolarimetry for V band (Takahashi et al., 2013) and the April result of Sterzik, Bagnulo, Palle (2012), but lower than Dollfus (1957) and the June result of Sterzik, Bagnulo, Palle (2012) by ∼2%.

In Fig. 7, obtained values of Θ are plotted against N, the directions normal to the scattering plane. The polarization position angles of a planetary reflection should be normal to the scattering plane in most phase angles. As expected, Θ almost coincides with N except for observations during lunar eclipse. This result is reasonable, and thus supports reliability of our observations and data reduction method.

4.–2. Comparison between the Waxing and Waning Phases

The data plots in Fig. 6 do not exhibit an apparent difference between the waxing and waning phases. To discuss more quantitatively, we fitted an scaled equation for Rayleigh scattering: $P(\alpha_e) = P_{\max}\sin^2\alpha_e/(1+\cos^2\alpha_e)$ (Equation (5.16) in Hapke, 1993) to the each of the waxing and waning phases. When all the data was used for the fitting, $P_{\max}$ of 7.7±0.4% and 8.5±0.7% were obtained for the waxing and waning phases, respectively. When the data on 2011-10-06 and 2012-03-15 were omitted from the fitting, $P_{\max}$ of 7.7±0.4% and 8.4±0.7% were derived, respectively. Although $P_{\max}$ for the waning phase are larger than that for the waxing phase, the difference is not significant. It is safe to say the enhancement in $P_{\max}$ for the waning phase is less than ∼ 1 %.

Table 3. **Results of the observations**

Moon phase	Date (UT)	$P \pm \sigma_P$ [%]	$\Theta \pm \sigma_\Theta$ [deg]
Waxing	2010-05-16	2.1 ± 1.4	171 ± 8
	2010-05-17	2.7 ± 0.5	175 ± 4
	2010-05-20	6.0 ± 0.9	11 ± 4
	2010-05-21	6.4 ± 1.1	12 ± 4
	2011-10-04	7.2 ± 0.8	168 ± 4
	2011-10-06	9.8 ± 4.5	5 ± 12
	2011-10-31	4.9 ± 0.5	167 ± 3
	2012-01-27	4.0 ± 0.4	146 ± 2
	2012-01-28	4.6 ± 0.9	142 ± 7
	2012-01-29	6.2 ± 2.3	143 ± 3
	2012-01-31	7.1 ± 1.8	152 ± 6
	2012-02-01	8.1 ± 2.2	159 ± 8
Waning	2010-06-03	7.1 ± 1.5	153 ± 6
	2010-06-09	3.7 ± 0.6	157 ± 4
	2010-09-02	7.6 ± 3.2	169 ± 9
	2011-09-22	5.4 ± 0.3	2 ± 2
	2011-12-18	7.5 ± 1.6	13 ± 7
	2011-12-19	6.2 ± 1.5	11 ± 9
	2012-03-15	12.7 ± 3.5	161 ± 8
Eclipse (east)	2011-12-10	1.4 ± 0.4	142 ± 9
Eclipse (west)	2011-12-10	1.2 ± 0.2	145 ± 8

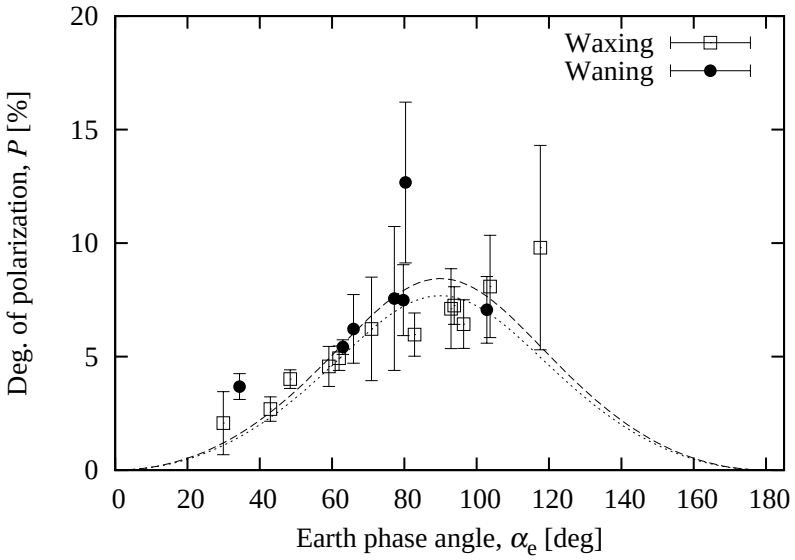

Fig. 6. **Plot of polarization degrees vs. Earth phase angles:** The dotted line is the best-fit curve to the data for the waxing phase and the dashed line for the waning phase. The data on 2011-10-06 ($P = 9.8 \pm 4.5\%$) and 2012-03-15 ($12.7 \pm 3.5\%$) were omitted from the fit due to the large errors.

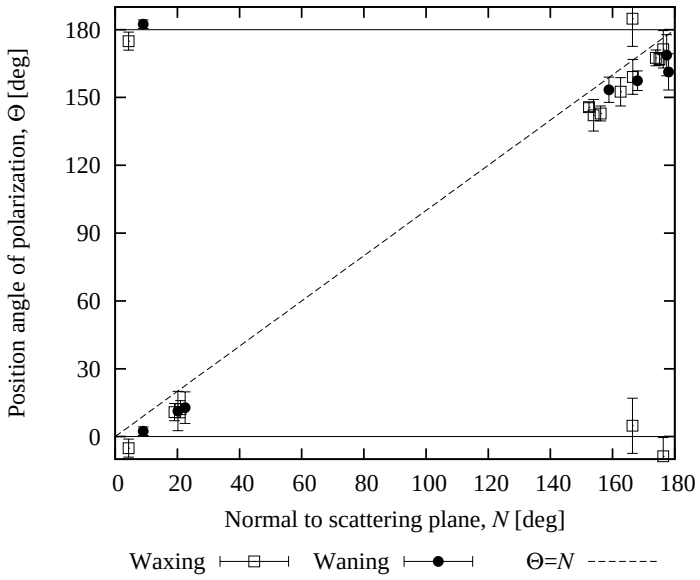

Fig. 7. **Plot of polarization position angles vs. the directions normal to the scattering plane:** $\Theta \pm 180°$ is also plotted to show the connection between $\Theta = 0°$ and $\Theta = 180°$.

As *Earthshine* is not *Earthlight* itself, the effect of lunar reflection on polarization should be considered to relate the observations to the Earth or Earth-like exoplanets. Lunar reflection does not add polarization because the Earth-Moon-Earth phase angle is zero (Coffeen, 1979). Instead, it depolarizes the polarized Earthlight. Dollfus (1957) estimated the depolarization factor as ∼3.3. This evaluation was based on a comparison of his optical polarimetric observations of Earthshine with the roughly estimated polarization degree of Earthlight, as well as on laboratory measurements of lunar samples.

Adopting the depolarization factor of ∼3.3, the maximum polarization degree of Earthlight in the V band is estimated to be ∼25%. This polarization is larger than other terrestrial planetary bodies in the Solar System (see Takahashi et al., 2013). Hence, the maximum polarization degree can be a clue to search an Earth-like exoplanet. The difference between polarization from a land-dominant surface and that from an ocean-dominant surface is evaluated to be less than ∼3%. Therefore, if we wish to detect a polarization enhancement due to ocean coverage, we should achieve a precision of at least one percent in direct polarimetry, though it is extremely challenging at present.

In McCullough's (2006) estimate, the polarization difference between a planet covered with an land surface and that with an ocean surface would be ∼ 15-20% for a condition of Earth-like cloud coverage. The ocean coverages in cloud-free area in our observations were averagely 40% and 85% for the waxing and waning phases, respectively. Simply assuming a linear response of the polarization difference to the ocean coverage, the upper limit we have driven corresponds to $\sim 7\%[\sim 3/(0.85 - 0.40)]$ for full land/ocean difference. The value is less than McCullough's (2006) value. This may be due to an underestimate of the cloud effect which dilutes the polarization enhancement by an ocean surface.

4.–3. Polarization during the Lunar Eclipse

During a lunar eclipse on 2011-12-10, polarization degrees of 1.4±0.4% and 1.2± 0.2% were measured for the celestial east and west sides of "Earthshine" on the Moon, respectively (Table 3). The position angles of polarization were $142° \pm 9°$ and $145° \pm 8°$, respectively, which were neither normal or parallel to the scattering. Polarization of Earthshine during lunar eclipses were previously reported by Coyne & Pellicori

(1969). The degree was 2.5% and the position angle was parallel to the scattering plane.

Although Earthshine in regular cases is originated from reflected light from the Earth, Earthshine during a lunar eclipse is from transmitted light through the atmosphere of the Earth. Polarization during a lunar eclipse may be attributed to (1) reflection on the Moon and/or (2) transmittance in the Earth atmosphere (before lunar reflection).

All the measurements of Earthshine and Moonshine are plotted in Fig. 8. No difference between Earthshine and Moonshine can be seen in both polarization degrees and position angles. This denies (2). Light reflected from some of airless solid bodies is known to exhibit a negative polarization (i.e, parallel to the scattering plane) at very small phase angles less then 2°, which is called polarization opposition effect (Mishchenko, 1993). This might explain the measured polarization during the lunar eclipse. Their typical degrees of the polarization opposition effect are 0.35% to 0.5% and position angles of polarization are parallel to the scattering plane (Lyot, 1929; Johnson et al., 1980; Rosenbush et al., 1997; Belskaya et al., 2002, 2003; Rosenbush & Kiselev, 2005; Rosenbush et al., 2006). However, the polarization degrees in our measurement are 1-2 % (Fig. 8a), and the position angles are not parallel to the scattering plane, rather independent of the plane (Fig. 8b). Therefore we should say that the observed polarization during the lunar eclipse is still puzzling.

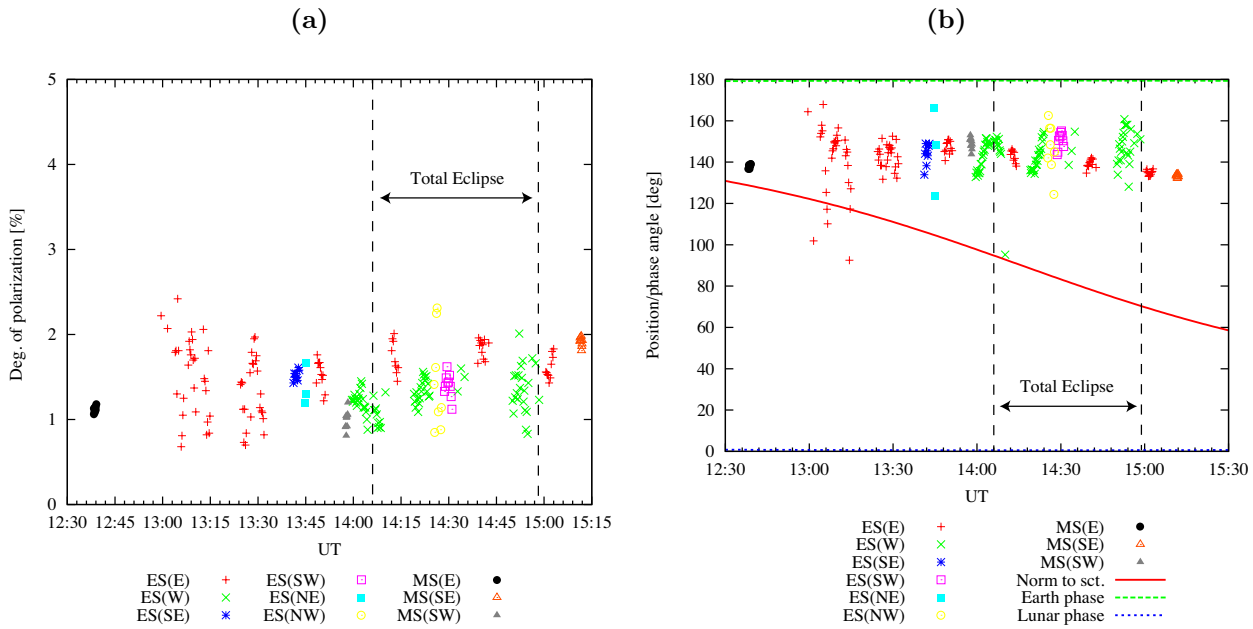

Fig. 8. **(a) Polarization degrees during the lunar eclipse on 2011-12-10:** ES and MS stand for Earthshine and Moonshine, respectively. The texts in parentheses signify observed positions written in celestial directions. The timeline of events in the eclipse is shown in Table 4 **(b) Polarization position angles during the lunar eclipse on 2011-12-10:** Legends are the same as Fig. 8a.

5. Conclusions

We conducted polarimetry of Earthshine on the Moon and compared the degree of polarization from a land-dominant surface and that from an ocean-dominant surface. Although a larger polarization by an ocean-dominant surface was implied, the difference was not significant. The upper limit of the difference was $\sim 1\%$ in Earthshine, which is interpreted as $\sim 3\%$ in Earthlight.

Table 4. **Timeline of the lunar eclipse on 2011-12-10** - This was calculated by Ephemeris Computation Office, Public Relations Center, National Astronomical Observatory of Japan

UT	Event
11:32	Beginning of the penumbral eclipse
12:45	Beginning of the partial eclipse
14:06	Beginning of the total eclipse
14:32	Maximum of the eclipse
14:58	End of the total eclipse
16:18	End of the partial eclipse
17:32	End of the penumbral eclipse

References

Arnold, L. 2008, Space Sci. Rev., 135, 323

Belskaya, I. N., Shevchenko, V. G., Efimov, Y. S., et al. 2002, Asteroids, Comets, and Meteors: ACM 2002, 500, 489

Belskaya, I. N., Shevchenko, V. G., Kiselev, N. N., et al. 2003, Icarus, 166, 276

Benner, S. A.,Ricardo, A.,Carrigan, M. A. 2004, Current Opinion in Chemical Biology, 8, 672

Coffeen, D. L. 1979, Journal of the Optical Society of America (1917-1983), 69, 1051

Coyne, G. V., & Pellicori, S. F. 1969, BAAS, 1, 215

Dollfus, A. 1957, Supplements aux Annales d'Astrophysique, 4, 3.

Hapke, B. 1993, Theory of reflectance and emittance spectroscopy(Cambridge University Press, Cambridge) ch.5

Hsu, J.-C., & Breger, M. 1982, ApJ, 262, 732

Fujita, K., Itoh, Y., & Mukai, T. 2009, Advances in Space Research, 43, 325

Johnson, P. E., Kemp, J. C., King, R., Parker, T. E., & Barbour, M. S. 1980, Nature, 283, 146

Lyot, B. 1929, Annales de 1'Observatoire de Paris, 8, 1 (translated as NASA Tech. Transl. TT-F-187, 1964)

McCullough, P. R. 2006, arXiv:astro-ph/0610518

Mishchenko, M. I. 1993, ApJ, 411, 351

Nishida, M. 2008, Kobe University master thesis

Pallé, E. 2010, EAS Publications Series, 41, 505

Rosenbush, V., Kiselev, N., & Avramchuk, V. 2006, J. Quant. Spectrosc. Radiat. Transfer, 100, 325

Rosenbush, V. K., Avramchuk, V. V., Rosenbush, A. E., & Mishchenko, M. I. 1997, ApJ, 487, 402

Rosenbush, V. K., & Kiselev, N. N. 2005, Icarus, 179, 490

Schmidt, G. D., Elston, R., & Lupie, O. L. 1992, AJ, 104, 1563

Sterzik, M. F., Bagnulo, S., & Palle, E. 2012, Nature, 483, 64

Takahashi, J., Itoh Y., Akitaya H., Okazaki A., Kawabata K., Oasa Y., & Isogai M. 2013, PASJ, 65, in press

Turnshek, D. A., Bohlin, R. C., Williamson, R. L., II, et al. 1990, AJ, 99, 1243

Zugger, M. E., Kasting, J. F., Williams, D. M., Kane, T. J., & Philbrick, C. R. 2010, ApJ, 723, 1168